ejpmr, 2021,8(5), 369-377

SJIF Impact Factor 6.222

EUROPEAN JOURNAL OF PHARMACEUTICAL AND MEDICAL RESEARCH

www.ejpmr.com

Research Article

ISSN 2394-3211

EJPMR

COMPREHENSIVE QSAR ANALYSIS AND COMPUTER ASSISTED MECHANISM STUDY OF CINNAMIC ACIDS AS POTENT ANTITUBERCULAR AGENTS

Jainendra Kumar B.[a], Suresh K.[b], Umarani W. A.[c], Sony Priya K.[c], Purna Nagasree K.[d] and Murali Krishna Kumar M.[c]*

[a]School of Pharmacy, Anurag Group of Institutions, Hyderabad, Telangana – 500088, India.
[b]Department of Microbiology, Gitam Institute of Science, Gitam (deemed to be university), Visakhapatnam – 530045.
[c]Pharmaceutical Chemistry Research Labs, AU College of Pharmaceutical Sciences, Andhra University, Visakhapatnam- Andhra Pradesh – 530003, India.
[d]Vignan Institute of Pharmaceutical Technology, Duvvada, Visakhapatnam, Andhra Pradesh – 530046, India.

***Corresponding Author: Dr. Murali Krishna Kumar M.**
Pharmaceutical Chemistry Research Labs, AU College of Pharmaceutical Sciences, Andhra University, Visakhapatnam- Andhra Pradesh – 530003, India.

Article Received on 02/03/2021 **Article Revised on 21/03/2021** **Article Accepted on 11/04/2021**

ABSTRACT

Cinnamic acids are one of the oldest class of natural products known to mankind. Along with varied bioactivities, these compounds are also known to possess antimicrobial activity. As these compounds possess αβ unsaturated carboxylic acid system similar to intermediates formed in fatty acid biosynthesis, it is hypothesized to interfere with enzymes involved in fatty acid biosynthesis. But there is no report of cinnamic acids interfering with the enzyme complex involved in human fatty acid biosynthesis (FAS-I), probably due to steric hindrance offered by the phenyl unit. But in case of *Mycobacterium tuberculosis*, very long chain fatty acids (mycolic acids) are biosynthesized by enzymes of FAS-II pathway. These enzymes are dissociated and relatively liberal in allowing larger substrates to participate in enzyme activity. Hence, we made an attempt to prepare and screen cinnamic acids for anti TB activity using MABA method and cell viability assays. Further we did a thorough docking simulation study on enzymes involve in FAS-II pathway with cinnamic acids. We found surprisingly high potency for the synthesized cinnamic acids (MIC 1.6 µg/mL). We also found the docking scores completely in agreement with our hypothesis of FAS-II enzyme inhibition as main mechanism of action. The bioactivity and SAR are discussed in detail.

KEYWORDS: Cinnamic acids, FAS-II inhibition, anti TB, *Mycobacterium tuberculosis.*

INTRODUCTION

Cell wall disruption remained in the forefront of antimicrobial drug discovery. More than 50% of antibiotics including betalactams, used clinically acts via inhibiting cell wall biosynthesis. *Mycobacterium tuberculosis*, the causative organism for tuberculosis, is a bacillus shielded by a unique thick lipid-rich cell wall.[1] The cellular envelope (Figure 1) is composed of peptidoglycan (PG), arabinogalactan (AG), and mycolic acids (MAs, long fatty acids i.e. C60-C90) and a lipopolysaccharide, lipoarabinomannan (LAM).[2,3]

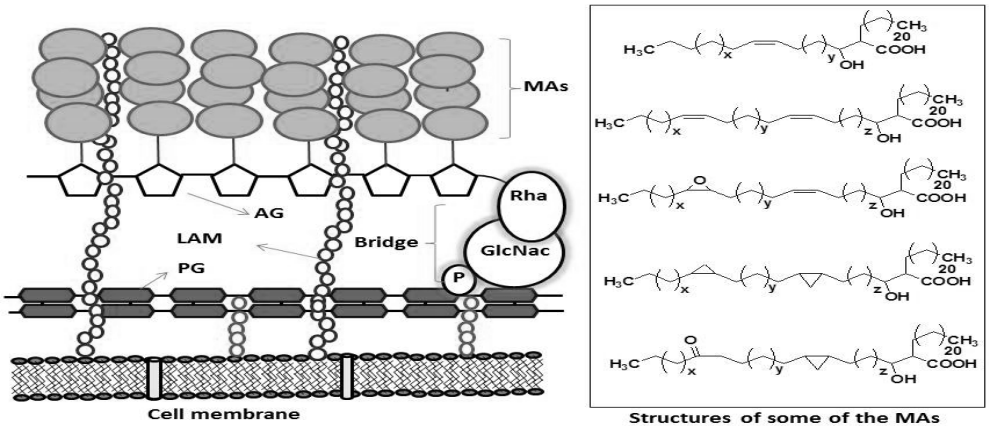

Figure 1: Cell envelope of *M. tuberculosis* with structural components.

The de novo fatty acid biosynthesis of C-14 to C-18 fatty acids in mammals and other higher organisms is catalyzed by a type I fatty-acid synthase (FAS-I), composed of a complex multifunctional polypeptide. In contrast, along with FAS-I, *M. tuberculosis* (Mtb) carries another important enzyme system FAS-II, the dissociated fatty-acid synthase composed of discrete enzymes. (**Figure 2**) The FAS-II takes long chain fatty acyl CoAs (C14-C24) as input to synthesize mycolic acids (C50-C60).[4-6]

Mycolic acids are biosynthesized by Claisen type condensation and reduction of C16 fatty acids.[7] The four distinct steps involved in the biosynthesis include synthesis of C24- C26 straight chain saturated fatty acids to provide C-1 and C-2 of the ά-alkyl chain; synthesis of the backbone of meromycolic acids of C40-C60; modification of meromycolic acids to introduce functional groups other than β-hydroxy; and the final condensation step to provide mycolic acids. Many enzymes involved in the catalysis of different steps in the biosynthesis of these molecules are targets to develop a mechanism based anti-TB drugs. Many of the genes in the mycolic acid biosynthesis have been identified and characterized.[7-9]

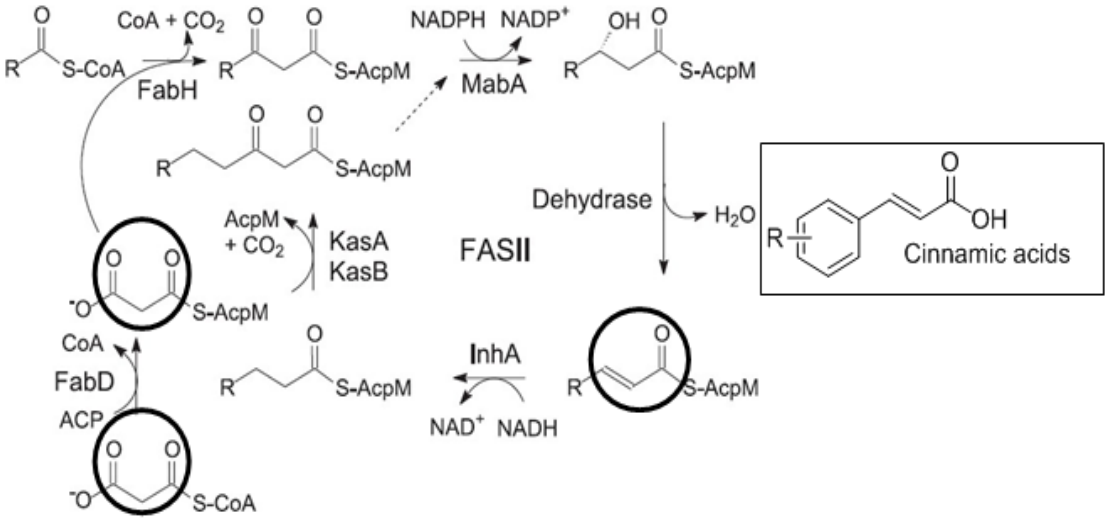

Figure 2: The type II fatty acid biosynthesis pathway (FASII) in *M. tuberculosis.*

In FAS-I system, the receptor pockets are tightly connected and have narrow channels to accommodate flexible lipid chains. But in the FAS-II system present in Mtb, the enzymes are dissociated and the receptor pockets are relatively large and relatively liberal in allowing access to structurally unrelated compounds. Hence it is planned to design compounds possessing these structural features. Cinnamic acids possess the α,β-unsaturated carbonyl moiety. Hence there is a great possibility for these compounds to interfere with the fatty acid synthesis via competitive inhibition. There are several reports indicating draggability of FAS-II enzymes.[10,11]

Clinical efficacy of cinnamic acids was first evaluated by Warbasse in 1894.[12] Here, TB infected rabbits survived for more than a year upon treatment with intravenous injection of cinnamic acid. Cinnamic acids are known for their antimicrobial, antioxidant and hepatoprotective activity.[13-15] Our research group has recently identified potent anti TB activity in natural hispolons, which possess the α,β-unsaturated carbonyl moiety.[16] Preliminary in vitro studies indicated fatty acid synthesis as the target for these compounds. Detailed synthesis, screening and docking simulations were conducted and the results are presented here.

MATERIALS AND METHODS

All the reagents used are of reagent grade. The reactions were monitored with silica gel TLC using appropriate mobile phase. Visualization of the spots was done either with the help of iodine chamber or by spraying 20% H_2SO_4 in ethanol followed by heating on a hot plate. The compound purity was also checked with silica gel TLC. Biotage Initiator system was used for Microwave reactions. Melting points were noted using EZMELT 120 (Stanford Research Systems, USA) and are uncorrected. IR spectral data is recorded either on Shimadzu FT-IR Affinity-1 system or Bruker ALPHA-T FTIR system using KBr pellet method. NMR spectral data was recorded on Bruker FT-NMR 400 MHz system in appropriate deuterated solvent using TMS as internal standard. Elemental analysis experiments were conducted using Carlo Erba elemental analyzer. ESIMS mass spectral studies were done on Agilent 6410 QQQ MS system. Computational studies were done on a Compaq Presario with 4GB RAM, 2.4GHz dual core processor. Molecular modeling was done using ChemBio Office 2012. Docking simulations were done using AUDocker LE, VINA. PyMol was used for docking analysis.

General procedure for the synthesis of cinnamic acids by Knoevenagel condensation.[17]

Scheme 1

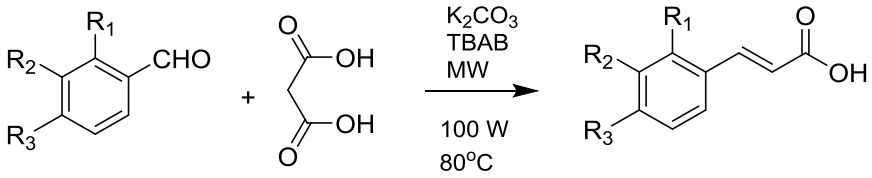

Code	R1	R2	R3	Code	R1	R2	R3
CA1	H	H	H	**CA10**	H	-OH	-OH
CA2	H	H	-OH	**CA11**	H	-Cl	H
CA3	H	-OCH3	-OH	**CA12**	H	-F	H
CA4	H	H	-OCH3	**CA13**	H	-Br	H
CA5	H	H	-OC2H5	**CA14**	H	-F	-F
CA6	H	H	-CH3	**CA15**	H	H	$-NO_2$
CA7	H	H	-F	**CA16**	H	$-NO_2$	H
CA8	H	H	-Br	**CA17**	-OCH3	H	-OCH3
CA9	H	H	-Cl	**CA18**	3-indolyl		

To a mixture of aromatic aldehyde or ketone (5 mmol), malonic acid (5 mmol), Tetrabutyl ammonium bromide (TBAB) (2.5 mmol) and K_2CO_3 (2.5 mmol) in a 10 ml reaction vessel, distilled water (5 mL) was added and crimped. The reaction mixture was subjected to microwave irradiation for 5 to 10 minutes using Biotage Initiator synthesizer (100W, 80^0C). After completion of the reaction as indicated by TLC, the reaction mixture was poured in ice cold water and acidified with dil. HCl. The product was isolated by filtration followed by washing with water. It was pure enough and further purified by crystallization from EtOAc: pet. ether or EtOH for carrying out spectral analysis.

Antimicrobial activity screening

The synthesized compounds (CA1-CA18) were tested for anti TB activity (according to NCCL standards 1985) against *Mycobacterium tuberculosis* H37Rv by Micro-plate Alamar Blue Assay (MABA).[18] Top nine potent compounds (CA2, CA7-CA10, CA14, CA18) that had shown potent anti TB activity (MIC 1.6 µg/mL) by MABA assay were further evaluated by MTT Assay[19] (cell proliferation Assay) and Axenic culture method against *Mycobacterium tuberculosis* MTB H37Ra (MTCC 300). In vitro Cytotoxicity studies by MTT Assay against different cell lines were carried out at a concentration of 10 µM.

Agar well-diffusion method[20] was followed to determine the antimicrobial activity on both gram positive (*Staphylococcus aureus* (NCIM 2122)) and gram-negative bacteria (*Escherichia coli* (NCIM 2137)). Antifungal activity of all the compounds was evaluated by the agar well diffusion method[21] against *Candida albicans* (NCIM 3102).

Computational studies

The 2D structures of the synthesized compounds were modeled using Chemdraw Ultra 10.0 (Cambridge software). The 2D models generated were then converted to 3D format using Chem3D ultra 10.0. The 3D models were finally subjected to energy minimization using molecular mechanics (MM2).

A number of potential protein targets were identified in *M. tuberculosis* but only few of them were isolated and identified. A total of four proteins were selected for this study based on their importance in key biochemical reactions and availability of flawless X-ray crystal structure in the Brookhaven Protein Data Bank (http://www.rcsb.org/pdb). We selected proteins whose structure was determined by x-ray diffraction (resolution ~2.05A^o) with a co-crystallized ligand. We also ensured that the structure is free from protein breaks. However, we considered Ramachandran plot statistics[22] as a very important filter for protein selection that < 1% of the residues fall in disallowed regions. Prior to optimization, polar hydrogens were added and network of hydrogen bond interactions were optimized by using MolProbity server.[23]

Software validation was performed in AutoDock Vina using the PDB structures of proteins Beta-Ketoacyl-Acyl Carrier Protein Synthase III (1HZP), KasA (5LD8), InhA (5MTP) and MabA (1UZN).[24] The prepared target protein is taken and docked with the bound co-crystallized ligand using the optimized docking parameters. The RMSD values of all atoms between the docked conformation (pose with best binding energy/DOCK score) and the conformation of the ligand present in the prepared protein were obtained by using YASARAview.[25] The RMSD values were found to be in the acceptable range (<2A^o) indicating that the parameters used for docking simulation are good in

reproducing X-ray crystal structure.[26]

The results obtained in the docking experiment were analyzed by using PyMol Molecular Graphics System (Ver 2.4.1). The lowest energy docked conformation of the ligand in the output file containing 10 best docked poses was selected and processed for necessary information and graphical presentation. The docked conformation was analyzed thoroughly for binding energy, hydrogen bond interactions, Vander Waals interactions and possible Π-Π interactions. In all these docking studies it is observed that cinnamic acids showed strong interactions with the amino acids in catalytic site of these enzymes.

RESULTS AND DISCUSSION

Synthesis of cinnamic acids

The IR spectrum of the cinnamic acids showed diagnostic signals for carboxylic acids (3300 cm-1 (broad, -COOH str) and 1670 cm^{-1} (-COOHstr)), aromatic ring (-C=C- 1610–1640 cm^{-1}). The ^{1}HNMR of CA1-CA18 showed signals for aromatic ring in the range δ 7.16 to 7.35. Characteristic signals of protons present on α,β-unsaturated carbonyl group at 6.4 (d, J=16Hz, α-H) and 7.6 (d, J=16Hz, β-H). The huge coupling constant confirmed formation of trans-cinnamic acid. The results obtained for elemental analysis or CHN analysis of the synthesized compounds is satisfactory (± 0.4% of required). Mass spectral data is in complete agreement with the assigned structures for the synthesized compounds.

CA1: Yield 85%. m.p.132°C. Anal. Found for $C_9H_8O_2$ (%): C 72.94, H 5.43 and O 21.58. ESIMS, (M-H) *m/z*: 147. IR, KBr pellet (γ, cm^{-1}): 1629 (C=C str), 1679 (C=O str), 3025 (Ar C-H str), 3446 (br, COOHstr). ^{1}H-NMR (δ, ppm): 6.43 (d, J = 16Hz, 1H), 7.39 (m, 3H), 7.52 (m, 2H), 7.69 (d, J = 16Hz, 1H), 10.01 (s, 1H).

CA2: Yield (%) 78. M.P. (°C) 214. Anal. Found for $C_9H_8O_3$: C 65.83, H 4.90 and O 29.23. ESIMS (M-H) *m/z*: 163. IR, KBr pellet (γ, cm^{-1}): 1625 (C=C str), 1665 (C=O str), 3028 (Ar C-H str), 3422 (br, COOHstr). ^{1}H-NMR (δ, ppm): 6.39 (d, J = 16Hz, 1H), 6.83 (d, J = 8Hz, 2H), 7.23 (d, J = 8Hz, 2H), 7.51 (d, J = 16Hz, 1H), 9.66 (s, 1H).

CA3: Yield (%) 92. M.P. (°C) 180. Anal. Found for $C_{10}H_{10}O_4$: C 61.84,H 5.18 and O 32.94. ESIMS (M-H) *m/z*:193. IR, KBr pellet (γ, cm^{-1}): 1150 (C-O str), 1630 (C=C str), 1671 (C=O str), 3005 (Ar C-H str), 2906 (Aliphatic CH str),3445 (br, COOHstr). ^{1}H-NMR (δ, ppm): 3.69 (s, 3H), 6.35 (d, J = 16Hz, 1H), 6.78 (d, J = 8Hz, 2H), 7.51 (d, J = 8Hz, 2H), 7.54 (d, J = 16Hz, 1H), 9.96 (s, 1H).

CA4: Yield (%) 90. M.P. (°C) 173. Anal. Found for $C_{10}H_{10}O_3$: C 67.40, H 5.65 and O 26.92. ESIMS (M-H) *m/z*: 177. IR, KBr pellet (γ, cm^{-1}): 1185 (C-O str), 1625 (C=C str), 1686 (C=O str), 3045 (Ar C-H str), 2930 (Aliphatic CH str), 3442 (br, COOHstr). ^{1}H-NMR (δ, ppm): 3.69 (s, 3H), 6.35 (d, J = 16Hz, 1H), 6.78 (d, J = 8Hz, 1H), 7.51 (d, J = 8Hz, 1H), 7.57 (d, J = 16Hz, 1H), 10.5 (s, 1H).

CA5: Yield (%) 90. M.P. (°C) 183. Anal. Found for $C_{11}H_{12}O_4$: C 63.44, H 5.80 and O 30.73. ESIMS (M-H) *m/z*: 207. IR, KBr pellet (γ, cm^{-1}): 1155 (C-O str), 1627(C=C str), 1673 (C=O str), 3018 (Ar C-H str), 2992 (Aliphatic CH str), 3444 (br, COOHstr). ^{1}H-NMR (δ, ppm): 1.39 (t, 3H), 4.05 (4, 2H), 6.51 (d, J = 14Hz, 1H), 6.93 (d, J = 8Hz, 2H), 7.18 (m, 2H), 7.74 (d, J = 14Hz, 1H), 10.9 (s, 1H).

CA6: Yield (%) 88. M.P. (°C) 197. Anal. Found for $C_{10}H_{10}O_2$: C 74.05, H 6.21 and O 19.72. ESIMS (M-H) *m/z*: 161. IR, KBr pellet (γ, cm^{-1}): 1629 (C=C str), 1678 (C=O str), 2986 (Aliphatic CH str), 3018 (Ar C-H str), 3439 (br, COOHstr). ^{1}H-NMR (δ, ppm): 2.97 (s, 3H), 6.29 (d, 14Hz, 1H), 6.79 (d, 8Hz, 2H), 7.41 (d, 14Hz, 1H), 7.68 (d, 8Hz, 2H), 9.67 (s, 1H).

CA7: Yield (%) 85 M.P. (°C) 210. Anal. Found for $C_9H_7FO_2$:C 65.05, H 4.24 and O 19.25. ESIMS (M-H) *m/z*: 165. IR, KBr pellet (γ, cm^{-1}): 1625 (C=C str), 1665 (C=O str), 3028 (Ar C-H str), 3422 (br, COOHstr). ^{1}H-NMR (δ, ppm): 6.47 (d, J = 16Hz, 1H), 7.23 (d, J = 8Hz, 1H), 7.75 (d, J = 8Hz, 1H), 7.57 (d, J = 16Hz, 1H), 10.9 (s, 1H).

CA8: Yield (%) 88 M.P. (°C) 262. Anal. Found for $C_9H_7BrO_2$:C 47.60, H 3.10 and O 14.08. ESIMS (M-H) *m/z*: 224. IR, KBr pellet (γ, cm^{-1}): 1618 (C=C str), 1668 (C=O str), 3025 (Ar C-H str), 3395 (br, COOHstr). ^{1}H-NMR (δ, ppm): 6.52 (d, 12Hz, 1H), 7.44 (d, 7Hz, 2H), 7.68 (d, 7Hz, 2H), 7.81 (d, 12Hz, 1H), 10.1 (s, 1H).

CA9: Yield (%) 80. M.P. (°C) 248. Anal. Found for $C_9H_7ClO_2$: C 59.19, H 3.85 and O 17.51. ESIMS (M-H) *m/z*: 181. IR, KBr pellet (γ, cm^{-1}): 1619 (C=C str), 1688 (C=O str), 3028 (Ar C-H str), 3445 (br, COOHstr). ^{1}H-NMR (δ, ppm): 6.67 (d, 16Hz, 1H), 7.43 (d, 8Hz, 2H), 7.55 (d, 8Hz, 2H), 7.79 (d, 14Hz, 1H), 10.8 (s, 1H).

CA10: Yield (%) 91. M.P. (°C) 213. Anal. Found for $C_9H_8O_4$: C 60.59, H 4.47 and O 35.51. ESIMS (M-H) *m/z*: 179. IR, KBr pellet (γ, cm^{-1}): 1158 (C-O str), 1618 (C=C str), 1685 (C=O str), 3013 (Ar C-H str), 3358 (br, COOHstr). ^{1}H-NMR (δ, ppm): 6.53 (d, 14Hz, 1H), 6.78 (d, 8Hz, 1H), 7.01 (m, 2H), 7.79 (d, 14Hz, 1H), 10.9 (s, 1H).

CA11: Yield (%) 90. M.P. (°C) 178. Anal. Found for $C_9H_7ClO_2$: C 59.19, H 3.85 and O 17.51. ESIMS (M-H) *m/z*: 181. IR, KBr pellet (γ, cm^{-1}): 1626 (C=C str), 1679 (C=O str), 3025 (Ar C-H str), 3398 (br, COOHstr). ^{1}H-NMR (δ, ppm): 6.55 (d, 14Hz, 1H), 7.35 (d, 8Hz, 1H), 7.48 (m, 2H), 7.59 (m, 1H), 7.75 (d, 14Hz, 1H), 10.5 (s, 1H).

CA12: Yield (%) 95. M.P. (°C) 165. Anal. Found for $C_9H_7FO_2$: C 65.05, H 4.24 and O 19.25. ESIMS (M-H) *m/z*: 165. IR, KBr pellet (γ, cm^{-1}): 1625 (C=C str), 1665 (C=O str), 3028 (Ar C-H str), 3425 (br, COOHstr). ^{1}H-NMR (δ, ppm): 6.59 (d, 12Hz, 1H), 7.13 (d, 6Hz, 1H), 7.34 (m, 3H), 7.82 (d, 12Hz, 1H), 11.5 (s, 1H).

CA13: Yield (%) 90. M.P. (°C) 177. Anal. Found for $C_9H_7BrO_2$: C 47.60, H 3.10 and O 14.07. ESIMS (M-H) *m/z*: 224. IR, KBr pellet (γ, cm^{-1}): 1628 (C=C str), 1665 (C=O str), 3032 (Ar C-H str), 3418 (br, COOHstr). ^{1}H-NMR (δ, ppm): 6.57 (d, 12Hz, 1H), 7.32 (d, 8Hz, 2H), 7.51 (m, 2H), 7.58 (m, 1H), 7.84 (d, 12Hz, 1H), 10.8 (s, 1H).

CA14: Yield (%) 80. M.P. (°C) 197. Anal. Found for $C_9H_6F_2O_2$: C 58.69, H 3.27 and O 17.36. ESIMS (M-H) *m/z*: 183. IR, KBr pellet (γ, cm^{-1}): 1622 (C=C str), 1664 (C=O str), 3019 (Ar C-H str), 3398 (br, COOHstr). ^{1}H-NMR (δ, ppm): 6.54 (d, 12Hz, 1H), 7.15 (d, 6Hz, 1H), 7.34 (m, 2H), 7.82 (d, 12Hz, 1H), 11.4 (s, 1H).

CA15: Yield (%) 85. M.P.(°C) 290. Anal. Found for $C_9H_7NO_4$: C 55.95, H 3.64 and O 33.1. ESIMS (M-H) *m/z*: 192. IR, KBr pellet (γ, cm^{-1}): 1635 (C=C str), 1695 (C=O str), 3014 (Ar C-H str), 3405 (br, COOHstr). ^{1}H-NMR (δ, ppm): 6.82 (d, 12Hz, 1H), 7.78 (d, 6Hz, 2H), 7.91 (d, 6Hz, 2H), 8.22 (d, 12Hz, 1H), 11.2 (s, 1H).

CA16: Yield (%) 80. M.P.(°C) 202. Anal. Found for $C_9H_7NO_4$: C 55.95, H 3.64 and O 33.12. ESIMS (M-H) *m/z*: 192. IR, KBr pellet (γ, cm^{-1}): 1629 (C=C str), 1689 (C=O str), 3018 (Ar C-H str), 3398 (br, COOHstr). ^{1}H-NMR (δ, ppm): 6.39 (d, J = 12Hz, 1H), 7.34 (m, 2H), 7.75 (d, 7Hz, 1H), 7.93 (dd, J = 2, 7Hz, 1H), 8.06 (d, J = 12Hz, 1H).

CA17: Yield (%) 80. M.P. (°C) 193. Anal. Found for $C_{11}H_{12}O_4$: C 63.43, H 5.80 and O 30.72. ESIMS (M-H) *m/z*: 207. IR, KBr pellet (γ, cm^{-1}): 1601 (C=C str), 1676 (C=O str), 2943 (aliphatic C-H str), 3003 (Ar C-H str), 3442 (br, COOHstr). ^{1}H-NMR (δ, ppm): 3.78 (s, 3H), 3.82 (s, 3H), 6.34 (d, 14Hz, 1H), 6.72 (m, 2H), 7.53 (d, 6Hz, 1H), 7.88 (d, 14Hz, 1H), 11.5 (s, 1H).

CA18: Yield (%) 90. M.P. (°C) 180. Anal. Found for $C_{11}H_9NO_2$: C 70.57, H 4.84 and O 17.07. ESIMS (M-H) *m/z*: 186. IR, KBr pellet (γ, cm^{-1}): 1622 (C=C str), 1664 (C=O str), 3019 (Ar C-H str), 3248 (NH str), 3392 (br, COOHstr). ^{1}H-NMR (δ, ppm): 6.49 (d, 12Hz, 1H), 7.06-7.17 (m, 2H), 7.51-7.55 (m, 3H), 7.62 (d, 12Hz, 1H), 11.4 (d, 12Hz, 1H).

Results for Antibacterial, antifungal and antitubercular activities

The synthesized compounds are screened for antibacterial, antifungal and antitubercular activity to obtain selective inhibitory profile of the synthesized compounds. Among the synthesized cinnamic acids (CA1-CA18); the compounds CA12 and 14 showed maximum potency with a zone of inhibition 16mm and 18mm against *S. aureus* and 10mm and 9mm against *E. coli* respectively. None of the tested compounds showed antifungal activity against *Candida albicans*. In case of antitubercular activity, CA2, CA7-CA10, CA14 and CA18 showed excellent anti TB activity by Microplate Alamar Blue Assay (MABA) against the *Mycobacterium tuberculosis* MTB H37Rv bacilli strain with an MIC 1.6 µg/ml. These compounds were further evaluated by using cell viability studies (Axenic and MTT assay, Table 2). In these studies, the compound CA10 showed maximum inhibitory activity of 86% (Axenic assay) and 84% (MTT assay) which is slightly better than the activity profile observed for rifampicin 84% (Axenic assay) and 83% (MTT assay). None of these compounds showed any cytotoxicity against HEK cell lines at a concentration 100µg/mL.

Structure activity relationships

At the outset cinnamic acids showed very potent antitubercular activity (Table 1) against the test organism *Mycobacterium tuberculosis* H37Rv. The MIC of the test compounds ranged from 1.6 to 25 µg/mL. In view of feeble activity observed against tested gram+ve/gram-ve bacteria and fungi, cinnamic acids showed highly selective inhibitory profile. As observed in the compounds CA2 and CA10, Substitution of benzene ring with -OH group at meta or para position potentiated anti TB activity of the compounds from 12.5 µg/mL.to 1.6 µg/mL As observed in CA3, CA4, CA5, CA6 and CA17 substitution of benzene ring with $-CH_3$, $-OCH_3$ or $-OC_2H_5$ significantly reduced the anti TB activity. The halogens Ci, Br and F equally improved the anti TB activity of cinnamic acid, when substituted at para position. But at meta position, none of these halogens could produce the MIC 1.6 µg/mL. Nitrogroup also failed to improve anti TB activity beyond 3.12 µg/mL. Addition of fluorine to 4-fluoro substituted cinnamic acid retained the potency. Replacement of benzene with 3-indolyl moiety surprisingly improved potency from MIC 12.5 to 1.6 µg/mL. More insight was obtained in the docking simulations to corroborate the observations we made in the *in vitro* studies.

Table 1: Zone of inhibition for anti-bacterial activity by cup plate method.

Sample code	ZI (mm)			MICµg/ml
	SA	***EC***	***CA***	MtbH37Rv
CA1	NA	NA	NA	12.5
CA2	8	NA	NA	**1.6**
CA3	NA	NA	NA	3.12
CA4	5	5	NA	6.25
CA5	5	5	NA	3.12
CA6	NA	8	NA	6.25
CA7	NA	5	NA	**1.6**
CA8	NA	NA	NA	**1.6**
CA9	5	NA	NA	**1.6**
CA10	6	5	NA	**1.6**
CA11	5	NA	NA	6.25
CA12	16	10	NA	3.12
CA13	9	6	NA	3.12
CA14	18	9	NA	**1.6**
CA15	NA	NA	NA	3.12
CA16	NA	NA	NA	3.12
CA17	NA	NA	NA	25
CA18	NA	NA	NA	**1.6**
Streptomycin (0.1mg/mL)	8	7		
Nystatin (1mg/mL)			18	
Pyrazinamide				3.12
Ciprofloxacin				3.12
Streptomycin				6.25

Table 2: Antitubercular activity results of *Mycobacterium tuberculosis* MTB H37Ra.

Compound code	% Inhibition (MTT Assay)	% Inhibition (Axenic Assay)
CA2	85%	77%
CA7	80%	80%
CA8	80%	79%
CA9	82%	80%
CA10	86%	84%
CA14	84%	84%
CA18	84%	79%
INH (Isoniazid, 10µ g/ml)	89%	92%
RIF (Rifampicin, 10µ g/ml)	84%	83%
Control (10µg/ml)	Nil	Nil

Computational studies

The docking simulations revealed strong interaction (Figure 3, Table 3) of cinnamic acids with four key enzymes involved in FAS-II. Docking simulations on mtFabH enzyme: The docking simulation studies of cinnamic acids on mtFabH clearly showed that the arylacrylate part of all the cinnamic acids fits snugly into the receptor pocket with –COOH group of these compounds showing strong interactions with the active site amino acids. Substitutions on aromatic ring, like –OH, -Cl and –F increased further polar interactions with other important amino acids like Asn247 and showed better docking scores. For example, the –COOH group of CA2 (MIC 1.6µg/mL; dock score ~8.3 Kcal/mol) and CA10 (MIC 1.6µg/mL; dock score ~8.4 Kcal/mol) showed strong hydrogen bond interactions with Asn274 and His244. In addition, they also showed interactions with nearby amino acids Tyr304, Asn247, Gly209. In case of the compound CA17, which showed poor bioactivity (MIC 25µg/mL), the 2, 4- methoxy group created steric hindrance by increasing the girth of the aromatic ring and that might have restrained access of active site amino acids to -COOH group of the cinnamic acids and resulted in dock score -6.5 K.cal/mol.

Docking simulations on MabA enzyme: The protein MabA, also named FabG1, has been shown to be part of fatty acid elongation system (FAS-II). It catalyzes the second step of an FAS-II elongation round, the NADPH-specific reduction of long chain β-ketoacyl derivatives.[92] Along with cinnamic acids all others showed docking scores 5.3 to 7.7 Kcal/Mol, indicating

less probability of MabA as the main protein target for the bioactivity.

Docking simulations on INHA enzyme: In InhA, the catalytic site contains NADH. Phe149, Tyr158 and Lys165 were found to play critical role in substrate recognition and reduction reaction. CA10, which showed excellent *in vitro* anti TB activity (MIC 1.6µg/mL) showed strong hydrogen bond interactions with Tyr158, Gln214 and NADPH. It also has shown salt bridge interactions with Pro156, stabilizing the catalytic loop. Similar observations were made for the remaining cinnamic acids.

Docking simulations on KasA enzyme: The –COOH group of the compound CA10 showed several strong hydrogen bond interactions with Cys171, His311 and His345 (figure 4.14). The catechol part of CA10 showed interactions with Gly406, Asp273, His276, Val278, Ala279 and Pro280. CA10 scored fairly well when compared with the co-crystallized ligand and thiolactomycin. Almost all cinnamic acids showed interactions with critical amino acids His311 and His345 present in the catalytic site.

The docking simulations clearly stated that the cinnamic acids are showing anti TB activity by interfering with multiple enzymes involved in fatty acid biosynthesis. Among the enzymes, mtFabH, KasA and InhA showed ligand binding energies proportional to the in vitro anti TB activity results. This *in silico* study further revealed critical structural requirements for optimal ligand interactions.

a)

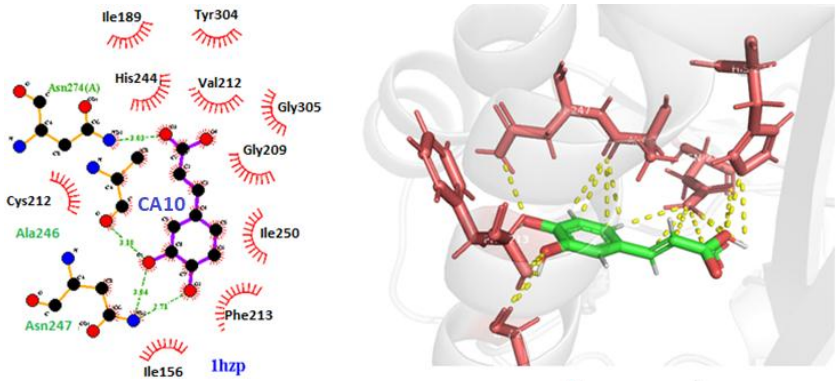

b)

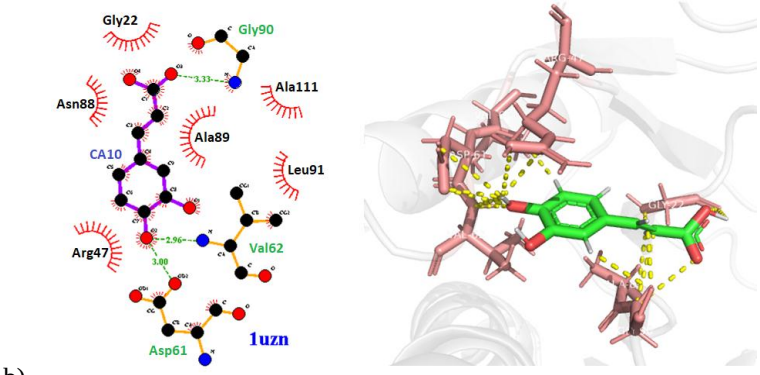

c)

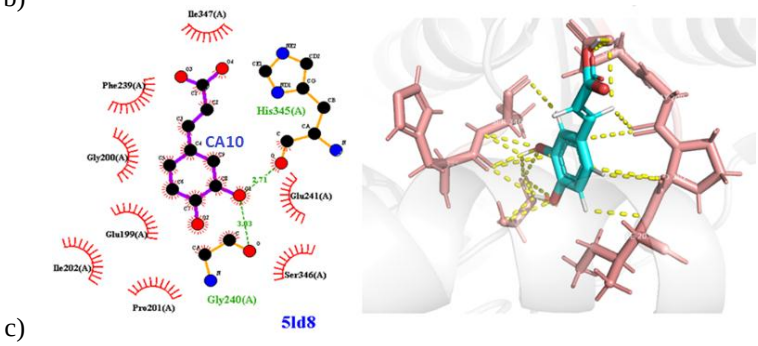

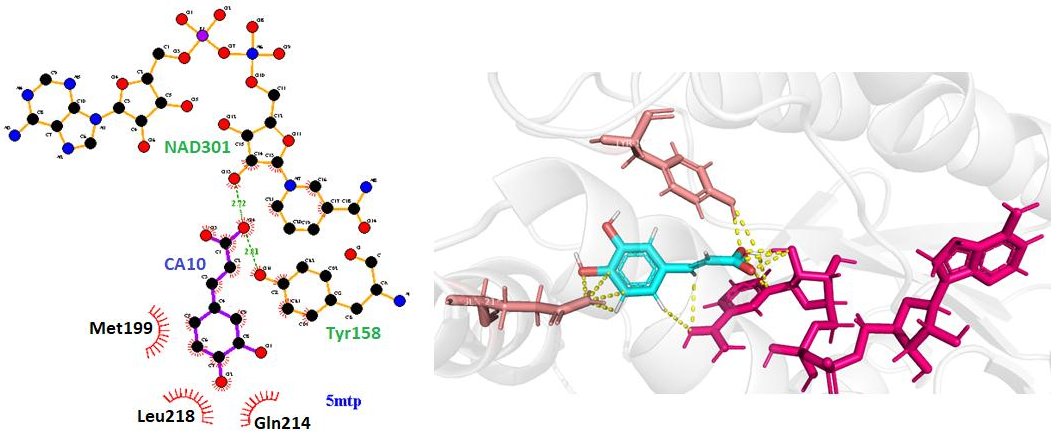

d)

Figure 3: Docking simulations of CA10 on FAS-II enzymes.
a) FabH b) MabA c) KasA and d) InhA

Table 3: DOCK scores (in Kcal/mol) of Cinnamic acids.

Ligand	FabH	MabA	InhA	KasA	MIC µg/ml
CA1	-6.3	-6.5	-7.7	-8.0	12.5
CA2	-8.3	-6.6	-7.7	-7.4	1.6
CA3	-7.2	-5.6	-7.8	-7.7	3.2
CA4	-6.9	-5.7	-7.8	-6.8	6.2
CA5	-7.3	-7.2	-7.7	-7.7	3.2
CA6	-7.4	-6.9	-8.5	-6.9	6.2
CA7	-7.8	-6.0	-8.1	-7.7	1.6
CA8	-8.0	-5.6	-7.2	-5.7	1.6
CA9	-8.4	-5.6	-7.3	-6.5	1.6
CA10	-8.4	-7.1	-8.6	-8.4	1.6
CA11	-7.3	-6.3	-8.0	-8.5	6.2
CA12	-7.1	-5.3	-7.9	-8.2	3.2
CA13	-7.8	-5.6	-7.1	-8.4	3.2
CA14	-7.9	-5.9	-8.3	-8.2	1.6
CA15	-7.8	-5.9	-8.6	-5.5	3.2
CA16	-7.5	-5.3	-8.1	-8.7	3.2
CA17	-6.5	-5.8	-7.4	-5.5	25
CA18	-7.0	-5.6	-8.1	-8.0	1.6

CONCLUSION

Cinnamic acids are easily accessible small molecule ligand used for development of different bioactive lead molecules. Here, we did in vitro and in silico studies to provide dependable insight into the antitubercular activity potential of cinnamic acids. Our research works resulted in identification of seven cinnamic acids showing potent and selective anti TB activity. Computational studies indicated that the enzymes FabH, InhA and KasA of the mycolic acid biosynthetic pathway as the probable molecular targets for their bioactivity.

Acknowledgements: Authors wish to thank the Director, NMR Research Center, Andhra University, Visakhapatnam for providing spectral data.

REFERENCES

1. Daffe M., Brennan P.J. and McNeil, M. Predominant structural features of the cell wall arabinogalactan of *Mycobacterium tuberculosis* as revealed through characterization of oligoglycosyl alditol fragments by gas chromatography/mass spectrometry and by 1H and 13C NMR analyses, J Biol Chem, 1990; 265: 6734-6743.
2. Rozwarski D.A., Vilcheze C., Sugantino M., Bittman R. and Sacchettini J.C. Crystal structure of the *M. tuberculosis* enoyl-ACP reductase, InhA, in complex with NADþ and a C_{16} fatty acyl substrate. J Biol Chem, 1999; 274: 15582-15589.
3. Azad A.K., Sirakova T.D., Fernandes N.D. and Kolattukudy P.E. Gene knockout reveals a novel gene cluster for the synthesis of a class of cell wall lipids unique to pathogenic *Mycobacteria*. J Biol Chem, 1997; 272: 16741–16755.
4. Marrakchi H., Laneelle G. and Quemard A. InhA, a target of the antituberculous drug isoniazid, is involved in a mycobacterial fatty acid elongation system, FAS-II. Microbiology, 2000; 146: 289-296.
5. Kremer L., Nampoothiri K. M., Lesjean S., Dover L.G., Graham S., Betts J., Brennan P.J., Minnikin D.E., Locht C. and Besra G.S. Biochemical characterization of acyl carrier protein (AcpM) and

malonyl-CoA:AcpM transacylase (mtFabD), two major components of *Mycobacterium tuberculosis* fatty acid synthase II. J Biol Chem, 2001; 276: 27967-27974.
6. Kremer L., Douglas J. D., Baulard A. R., Morehouse C., Guy M.R., Alland D., Dover L.G., Lakey J.H., Jacobs W.R. Jr., Brennan P.J., Minnikin D.E. and Besra G.S. Thiolactomycin and related analogues as novel anti-mycobacterial agents targeting KasA and KasB condensing enzymes in *Mycobacterium tuberculosis*. J Biol Chem, 2000; 275(22): 16857-16864.
7. Portevin D., De Sousa-D'Auria C., Houssin C., Grimaldi C., Chami M., Daffe M. and Guilhot C. A polyketide synthase catalyzes the last condensation step of mycolic acid biosynthesis in *mycobacteria* and related organisms. Proc Natl Acad Sci USA, 2004; 101(1): 314–349.
8. Fitzmaurice A.M. and Kolattukudy P.E., An acyl-CoA synthase (acoas) gene adjacent to the mycocerosic acid synthase (mas) locus is necessary for mycocerosyl lipid synthesis in *M.tuberculosis* var. bovis BCG. J Biol Chem, 1998; 273: 8033–8039.
9. Takayama K., Wang C. and Besra G.S. Pathway to Synthesis and Processing of Mycolic Acids in *Mycobacterium tuberculosis.* Clin Microbiol Rev, 2005; 18(1): 81-101.
10. Mdluli K., Slayden R. A., Zhu Y., Ramaswamy S., Pan X., Mead D., Crane D. D., Musser J. M. and Barry C. E. III. Inhibition of a *Mycobacterium tuberculosis beta*-ketoacyl ACP synthase by isoniazid. Science, 1998; 280(5369): 1607-1610.
11. Moustafa G.A.I., Nojima S., Yamano Y., Aono A., Arai M., Mitarai S., Tanaka T. and Yoshimitsu T. Potent growth inhibitory activity of (±)-platencin towards multi-drug- resistant and extensively drug-resistant *Mycobacterium tuberculosis*. Med Chem Comm, 2013; 4: 720-723.
12. Warbasse J.P. Cinnamic acid in the treatment of tuberculosis. Ann. Surg., 1894; 19(1): 102-117.
13. Natella F., Nardini M., Felice D.M. and Scaccini C., Benzoic and cinnamic acid derivatives as antioxidants: structure-activity relation, J Agric Food Chem., 1999; 47(4): 1453– 1459.
14. Sal'nikova S.I., Dorogovoz S.M., Slyshkov V.V. and Guzhva N.N. Hepatoprotective activity of analogs of cinnamic acid. Pharmol Toxicol, 1989; 52(3): 77-80.
15. Pérez-Alvarez V., Bobadilla R.A. and Muriel P. Structure–hepatoprotective activity relationship of 3,4-dihydroxycinnamic acid (caffeic acid) derivatives. J Appl Toxicol, 2001; 21(6): 527-31.
16. Subbaraju G.V., Balaji N.V., Hari babu B., Nagasree K.P. and Kumar M.M.K. Synthesis, screening and docking analysis of hispolon analogs as potential antitubercular agents, Bioorg and Med Chem Lett, 2017; 27(1): 11-15.
17. Gupta M. and Wakhloo B.P., Tetrabutylammoniumbromide mediated Knoevenagel condensation in water: synthesis of cinnamic acids, Arkivoc, 2007; 94-98.
18. Franzblau S.G., Witzig R.S., Mclaughlin J.C., Torres P., Madico G., Hernandez A., Degnan M.T., Cook M.B., Quenzer V.K., Ferguson R.M. and Gilman R.H. Rapid, low-technology MIC determination with clinical *Mycobacterium tuberculosis* isolates by using the microplate Alamar Blue assay, J Clin Microbiol, 1998; 36(2): 362-366.
19. Gonzalez R. J. and Tarloff J.B., Evaluation of hepatic subcellular fractions for Alamar blue and MTT reductase activity. Toxicol In Vitro, 2001; 15: 257-259.
20. Valgas C., De Souza S.M., Smania E.F.A. and Smania A.Jr., Screening methods to determine antibacterial activity of natural products. Braz J Microbiol, 2007; 38(2): 369–380.
21. Magaldi S., Mata Essayag S., de Capriles Perez, C., Colella M.T., Olaizola C. and Ontiverus Y. Well diffusion for anti-fungal susceptibility testing. Int J Infect Dis, 2004; 8(1): 39-45.
22. http://mordred.bioc.cam.ac.uk /~rapper/rampage.php,
23. http://molprobity.biochem.duke.edu/index.php
24. Trott O. and Olson A. J., AutoDock Vina: improving the speed and accuracy of docking with a new scoring function, efficient optimization and multithreading, J Comp Chem., 2010; 31: 455-461.
25. http://www.yasara.org/viewdl.htm
26. Vieth M., Hirst J.D., Kolinski A. and Brooks C.L. Assessing energy functions for flexible docking. J Comput Chem, 1998; 19(14): 1612-22.